Available online at www.sciencedirect.com

ScienceDirect

Palaeoworld 28 (2019) 550–561

Palaeoworld

www.elsevier.com/locate/palwor

The bony labyrinth of *Platecarpus* (Squamata: Mosasauria) and aquatic adaptations in squamate reptiles

Hongyu Yi [a,b,c,*], Mark Norell [c]

[a] *Key Laboratory of Vertebrate Evolution and Human Origins, Institute of Vertebrate Paleontology and Paleoanthropology, Chinese Academy of Sciences, Beijing, 100044, China*

[b] *CAS Center for Excellence in Life and Paleoenvironment, Beijing, 100044, China*

[c] *American Museum of Natural History, New York, NY, USA*

Received 10 June 2018; received in revised form 23 October 2018; accepted 7 December 2018
Available online 15 December 2018

Abstract

Mosasaurs were among the last marine reptiles that lived before the Cretacesous–Paleogene extinction. Little is known about the sensory evolution of mosasaurs in relation to their aquatic lifestyle. In this study, the braincase of *Platecarpus* was CT-scanned and virtual models were constructed showing the bony labyrinth — or the inner ear — a sensory apparatus for balance and hearing. The virtual inner ear consists of the semicircular canals, vestibule, and cochlea. Compared with extant squamates, *Platecarpus* resembles sea snakes in having a small vestibule with a flat dorsal surface, but it differs from non-mosasaurian squamates in having rounded semicircular canals. Phylogenetic linear regression analysis supports a linear relationship, independent from phylogeny, between the length of the three semicircular canals and the length of the skull. The semicircular canals of *Platecarpus* are shorter than predicted, but the fossil data fell within the 95% prediction interval calculated from the extant data and the skull length of *Platecarpus*. Although size reduction of the bony labyrinth has been associated with aquatic adaptions in mammals, our results suggest that in squamates, semicircular canal size is related to skull size rather than habitat preference.

Keywords: Mosasaur; Bony labyrinth; X-ray computed tomography; Aquatic adaptation; Squamate; Reptile

1. Introduction

Mosasaurs were extinct "marine lizards", a group of squamate reptiles reaching their highest diversity in the Late Cretaceous (Russell, 1967). Unlike modern sea snakes, they became fully aquatic yet retained axial appendages. Mosasaurs evolved from terrestrial lizards (Conrad, 2008; Gauthier et al., 2012), similarly to the origin of cetaceans from terrestrial mammals. In relation to habitat shift, mosasaurs evolved flippers and flat tails to aid swimming (Russell, 1967). Advanced mosasaurs were fully aquatic, with fossil evidence suggesting that they were live-bearing (Caldwell and Lee, 2001).

Compared with the mosasaur postcranial skeleton, less is known about the evolution of their sensory systems in the adaption to a fully aquatic lifestyle. Russell (1967) studied the inner ear of mosasaurs, an organ in the braincase that senses speed and balance, as well as environmental sound (Wever, 1978). The bony wall of the soft-tissue inner ear is termed the bony labyrinth whose canals can be revealed in disarticulated braincases. Disarticulated bones of the mosasaur braincase were used by Russell (1967) who described the bony labyrinth as similar to varanoid lizards. With the development of high resolution X-ray CT techniques, recent studies have generated three-dimensional virtual models of the bony labyrinth of mosasaurs (Georgi, 2008; Cuthbertson et al., 2015; Yi and Norell, 2015), showing the semicircular canals and vestibule were considerably different from the condition in varanoids.

The bony labyrinth of *Platecarpus* was first described by Georgi (2008) using CT data from a medical scanner. One three-dimensional virtual model was reconstructed for *Platecarpus*

* Corresponding author at: Key Laboratory for Vertebrate Evolution and Human Origins, Institute of Vertebrate Paleontology and Paleoanthropology, Chinese Academy of Sciences, Beijing 100044, China.
E-mail address: yihongyu@ivpp.ac.cn (H. Yi).

https://doi.org/10.1016/j.palwor.2018.12.001

(Georgi, 2008) based on the braincase of AMNH FARB1645, but the cochlear region was not visible. This study re-scanned this braincase using an industrial-grade high-energy X-ray and customizable scanning parameters. This increased the contrast of the fossil material to the rock matrix and enabled us to segment the whole vestibule and cochlea of *Platecarpus*.

The size of semicircular canals has been shown to be reduced in cetacean mammals, which has been suggested to reduce their sensitivity to fast rotations in the water (Spoor et al., 2002). Studies on the size of the bony labyrinth in marine squamates have shown mixed signals. Polcyn (2008) reported markedly reduced bony labyrinths in mosasaurs, compared with terrestrial varanoids, yet a recent quantitative analysis on *Plioplatecarpus* bony labyrinth (Cuthbertson et al., 2015) failed to find statistical support for shorter semicircular canals than in extant squamates, proportional to the length of the skull. Here we compared the streamlined lengths of the three semicircular canals of *Platecarpus* with 49 extant squamate species using phylogenetic generalized linear regressions.

Institutional abbreviations: AMNH FARB, American Museum of Natural History collection of Fossil Amphibians Reptiles and Birds; AMNH R, American Museum of Natural History collection of extant Reptiles; FMNH, Field Museum of Natural History; USNM, United States National Museum, Smithsonian Institution; TNHC, Texas Natural History Collections, University of Texas at Austin.

2. Materials and methods

2.1. Material

Two fossil specimens of *Platecarpus* were scanned in this study: AMNH FARB1566 and AMNH FARB1645. Both specimens were identified as *Platecarpus coryphaeus* (Cope, 1872; Russell, 1967), but recent studies synonymized *P. coryphaeus* with *P. tympaniticus* (Konishi and Caldwell, 2007; Lindgren et al., 2010). The braincase of each specimen was CT scanned to reconstruct the otic region. Extant squamates were sampled to compare with the fossil material, including 49 extant species representing various sizes and habitats (Table 1). Habitats of the sampled taxa include aquatic, semi-aquatic, terrestrial generalists, and terrestrial burrowing. The habitat groups indicates the major ecological preference of extant species, as described in Greene (2000), Pianka and Vitt (2006), IUCN (2017), and The Reptile Database (http://www.reptile-database.org, edited by Uetz, P., Freed, P., Hošek, J., accessed 2018).

2.2. CT scanning

All specimens were scanned using a GE phoenix v|tome|x s 240 scanner. Two scan strategies were used: the "high-voltage" strategy and the "high-current" strategy. Scanning fossilized materials requires high-energy X-ray to ensure that the beams can penetrate the whole sample, which can be reached by increasing the scanning voltage or current. For extremely dense specimens the use of high voltage enables the X-ray to penetrate the matrix, but this collects little information to distinguish density variations in the low-density areas. Using a lower voltage, the X-ray may not be powerful enough to penetrate the ultra-dense regions, but more resolution is gained on most parts of the fossil specimen.

From preliminary scans of the fossil specimens, we observed in the otic regions ultra-dense concretions that blurred the surrounding vestibular area in the scan images. To better image the vestibule and semicircular canals, which is medium to high in the density profile, we experimented with several different scanning parameters (Table 2).

2.3. Measurements of inner ear and skull size

The semicircular canals are curved tubes in shape (Fig. 1). In previous studies, length of the semicircular canals was measured in two-dimensional planar images best fitted to the three-dimensional canals (Georgi, 2008; Cuthbertson et al., 2015). In this study, the length of the semicircular canals was measured on the outer surface from the point the canal connects with the common crus to the point it connects with the ampulla (Fig. 1A, B). The three-dimensional streamline length of semicircular canals was taken in VG Studio Max 2.2. The length of the skull was measured in its sagittal plane between the anterior tip of the premaxilla and the mid-point of the posterior margin of the parietal (Fig. 1C). For extant species, the length of the skull was measured on three-dimensional virtual models using VG Studio Max 2.2. For *Platecarpus*, the length of the skull was estimated from the width of the skull, assuming homogeneous growth of the skull in the two directions. The skull length of AMNH FARB1645 was extrapolated from the data of four extant *Varanus* skulls (Table 3).

2.4. Size analysis of the bony labyrinth

Phylogenetic generalized linear regression was performed on extant samples to test whether the length of semicircular canals is linear to skull length, taking into account phylogenetic relationships (Freckleton et al., 2002; Felsenstein, 2004). Phylogenetic relationships of the sampled taxa (Fig. 2) were determined following previous global analyses of squamate phylogeny (Pyron et al., 2013), as well as Reeder et al. (2015) for mosasaur position and Sanders et al. (2013) for sea snake inter-relationships. All branch lengths were set to 1 for phylogenetic generalized linear regression analysis. Where linear relationship is significant and independent from the phylogeny, a regular linear regression line was fitted to the extant data. For *Platecarpus*, the length of the semicircular canals was compared with the predicted data with a 95% prediction interval using the regression model of extant species. All analyses were performed in R following conventional procedures (R Core Team, 2016).

2.5. Calculation on the linear relationship between semicircular canal length and skull length

Jones and Spells (1963) suggested a linear relationship between the logarithm of the radius of semicircular canals (R)

Table 1
List of species sampling.

Species	Specimen number	Fossil/extant	Habitat	Source of raw CT data
Platecarpus tympaniticus	AMNH FARB1566	Fossil	Aquatic	Original
Platecarpus tympaniticus	AMNH FARB1645	Fossil	Aquatic	Original
Aipysurus eydouxi	AMNH R14169	Extant	Aquatic	Original
Aipysurus laevis	AMNH R5087	Extant	Aquatic	Original
Aipysurus duboisii	AMNH R161749	Extant	Aquatic	Original
Emydocephalus annulatus	AMNH R4998	Extant	Aquatic	Original
Disteria stokwesii	AMNH R12578	Extant	Aquatic	Original
Hydrophis ornatus	AMNH R161770	Extant	Aquatic	Original
Hydrophis caerulescens	AMNH R86181	Extant	Aquatic	Original
Laticauda laticaudata	AMNH R161778	Extant	Aquatic	Original
Laticauda colubrina	AMNH R28996	Extant	Aquatic	Original
Laticauda semifasciata	AMNH R161779	Extant	Aquatic	Original
Acrochordus javanicus	AMNH R92269	Extant	Aquatic	Original
Lanthanotus borneensis	AMNH R113983	Extant	Semi-aquatic	Original
Amblyrhynchus cristatus	AMNH R147812	Extant	Semi-aquatic	Original
Chamaeleo calyptratus	AMNH R11120	Extant	Generalist	Original
Ophisaurus ventralis	AMNH R22432	Extant	Generalist	Original
Heloderma suspectum	AMNH R161167	Extant	Generalist	Original
Anguis fragilis	AMNH R21745	Extant	Generalist	Original
Varanus indicus	AMNH R58389	Extant	Generalist	Original
Varanus salvator	AMNH R94538	Extant	Generalist	Original
Varanus salvadorii	AMNH R59873	Extant	Generalist	Original
Varanus komodoensis	AMNH R74607	Extant	Generalist	Original
Lampropeltis getulus	AMNH R95965	Extant	Generalist	Original
Pareas hamptoni	AMNH R153711	Extant	Generalist	Original
Lamprophis lineatus	AMNH R50646	Extant	Generalist	Original
Corallus caninus	AMNH R55910	Extant	Generalist	Original
Python molurus	TNHC[a]	Extant	Generalist	DigiMorph
Naja naja	FMNH 22468	Extant	Generalist	DigiMorph
Eunectes murinus	AMNH R29349	Extant	Generalist	Original
Trimeresurus stejnegeri	AMNH R21057	Extant	Generalist	Original
Echiopsis curta	AMNH R115397	Extant	Generalist	Original
Ptyas mucosa	AMNH R33243	Extant	Generalist	Original
Boiga irregularis	AMNH R69292	Extant	Generalist	Original
Pygopus nigriceps	AMNH R161427	Extant	Generalist	Original
Anniella pulchra	AMNH R12851	Extant	Burrowing	Original
Cylindrophis maculatus	AMNH R126605	Extant	Burrowing	Original
Uropeltis ceylanica	AMNH R43344	Extant	Burrowing	Original
Typhlops jamaicensis	USNM 12378	Extant	Burrowing	DigiMorph
Eryx colubrinus	FMNH 63117	Extant	Burrowing	DigiMorph
Anilius scytale	USNM 204078	Extant	Burrowing	DigiMorph
Loxocemus bicolor	FMNH 104800	Extant	Burrowing	DigiMorph
Heterodon platirhinos	FMNH 194529	Extant	Burrowing	DigiMorph
Simoselaps bertholdi	AMNH R115427	Extant	Burrowing	Original
Rhinotyphlops caecus	AMNH R05844	Extant	burrowing	Original
Sonora semiannulata	AMNH R170522	Extant	Burrowing	Original
Exiliboa placata	AMNH R102892	Extant	Burrowing	Original
Xenopeltis unicolor	AMNH R161693	Extant	burrowing	Original
Typhlosaurus lineatus	AMNH R98481	Extant	Burrowing	Original
Bipes canaliculatus	AMNH R113487	Extant	Burrowing	Original
Dibamus novaeguineae	AMNH R86710	Extant	Burrowing	Original

[a] The specimen is to be accessioned.

and body mass (m), from which they deduced the following equation:

$$\log_{10}100\mathrm{R} = 0.0761\,(\pm 0.0402)\log_{10}\mathrm{m} + 2.3797$$

Therefore, the logarithm of R is linear to the logarithm of m:

$$\log R \propto \log m$$

R is hard to measure in squamates, as the semicircular canals are not circular in shape, but the circumference of a circle (Csc) is linear to R^2. The logarithm of C is linear to that of R:

$$\log Csc \propto 2\log R \propto \log m$$

The body mass is proportional to the body volume, assuming the density of vertebrates is similar among closely related taxa. The volume of the body is a product of the length (Lb), width

Table 2
Scanning parameters for the two fossil specimens.

	Parameter	AMNH FR1645	AMNH FR1566
Scan 1: high-voltage	Voltage (kv)	200	210
	Current (mA)	190	200
	Timing (ms)	333	333
	Magnification	×2.00574006	×3.24546449
Scan 2: high-current	Voltage (kv)	170	170
	Current (mA)	310	320
	Timing (ms)	333	333
	Magnification	×3.72350912	×3.56225895

(Wb) and height (Hb), if the body is considered as a cuboid between the tip of the snout and the cloacal opening at the base of the tail. Because body mass is proportional to body volume and proportional to the body length tripled, logarithm of m is linear to the log of body dimensions:

$$\log m \propto 3 \log Lb \propto 3 \log Wb \propto 3 \log Hb$$

Because log*Csc* is linear to log*m*, it is linear to log*Lb*:

$$\log Csc \propto \log Lb$$

The last formula shows a linear relationship between the logarithm of semicircular canal circumference (Csc) and body length (Lb). This study implemented an additional presumption: body length (Lb) is proportional to skull length (Lsk); therefore, the formula used in this study is as following:

$$\log Csc \propto \log Lsk$$

This study uses observed values of the semicircular canal length and skull length to test the above linear relationship in squamates. Using the extant data, we further predicted the semicircular canal length for *Platecarpus* given its skull length.

3. Results

3.1. CT scanning and quality improving

All mosasaur fossils scanned in this study contain several regions of ultra-high density material, especially in the otic region. Density differences between the concretions and the surrounding braincase are dramatic — much larger than what is expected for fossilized otoliths. The concretions were also found in areas other than the otic region, e.g., inside the basisphenoid in AMNH FARB1566 (Fig. 3E, G).

When imaging the otic region using X-ray, these bright regions blur the edge of semicircular canals. For specimens containing ultra-dense regions, the scan quality was improved by using high current (Fig. 3). In the high-current scan, the semicircular canals of AMNH FARB1645 shows a clear margin (Fig. 3A, B), whereas in the high-voltage scan, the margin is blurred from the adjacent ultra-bright concretion (Fig. 3C, D). Similar results were gained for AMNH FARB1566 (Fig. 3E–H).

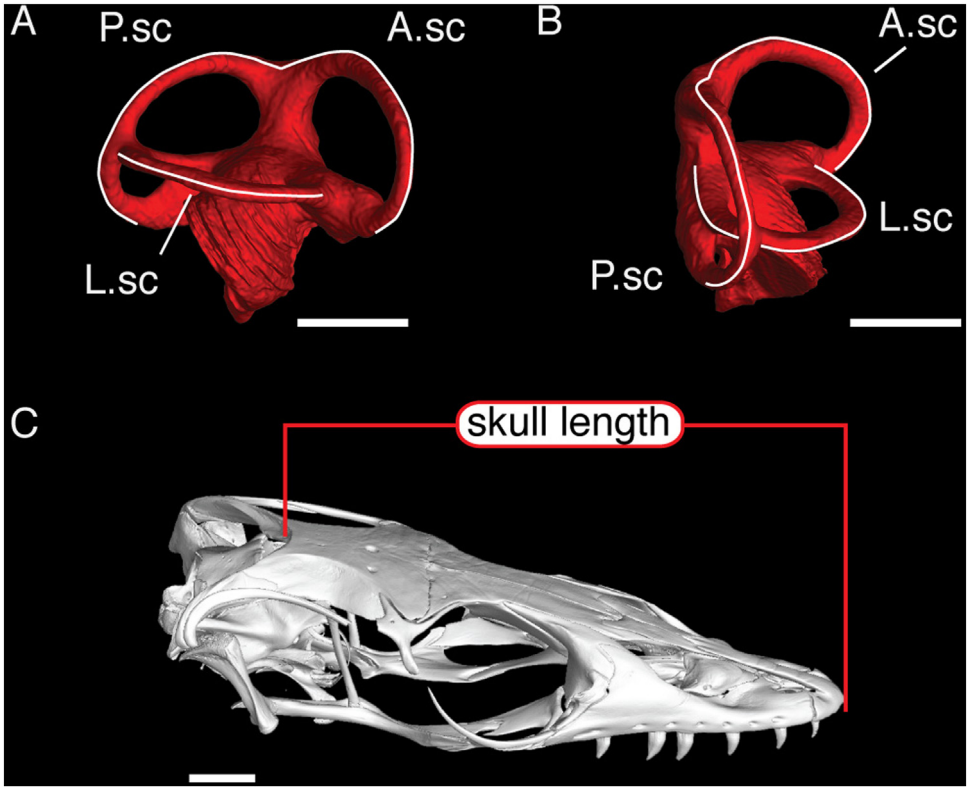

Fig. 1. Length measurements of the semicircular canals and the skull. (A, B) Measuring the length of semicircular canals by fitting three-dimensional lines to the external surface of each canal; the ear model is reconstructed from AMNH FARB1645. (C) Skull length was taken between the snout tip to the middle of the posterior margin of the parietal along the sagittal plane, as shown in the reconstructed skull of *Varanus indicus* (AMNH R58389). A.sc, length of the anterior semicircular canal; L.sc, length of the lateral semicircular canal; P.sc, length of the posterior semicircular canal. Scale bar = 5 mm.

Table 3
Measurements of extant *Varanus* skulls and the estimated skull length of AMNH FARB1645.

	Skull length (mm)	Skull width between paroccipital processes (mm)
Varanus komodoensis	174.06	77.55
Varanus salvadorii	127.41	42.98
Varanus salvator	83.18	34.64
Varanus indicus	40.55	17.04
AMNH FARB1645 (fossil)	363.41*	160.52
Linear model of extant data	Skull length = 2.19 × skull width + 12.07 $R^2 = 0.94$	

* Denotes the estimated skull length of AMNH FARB1645.

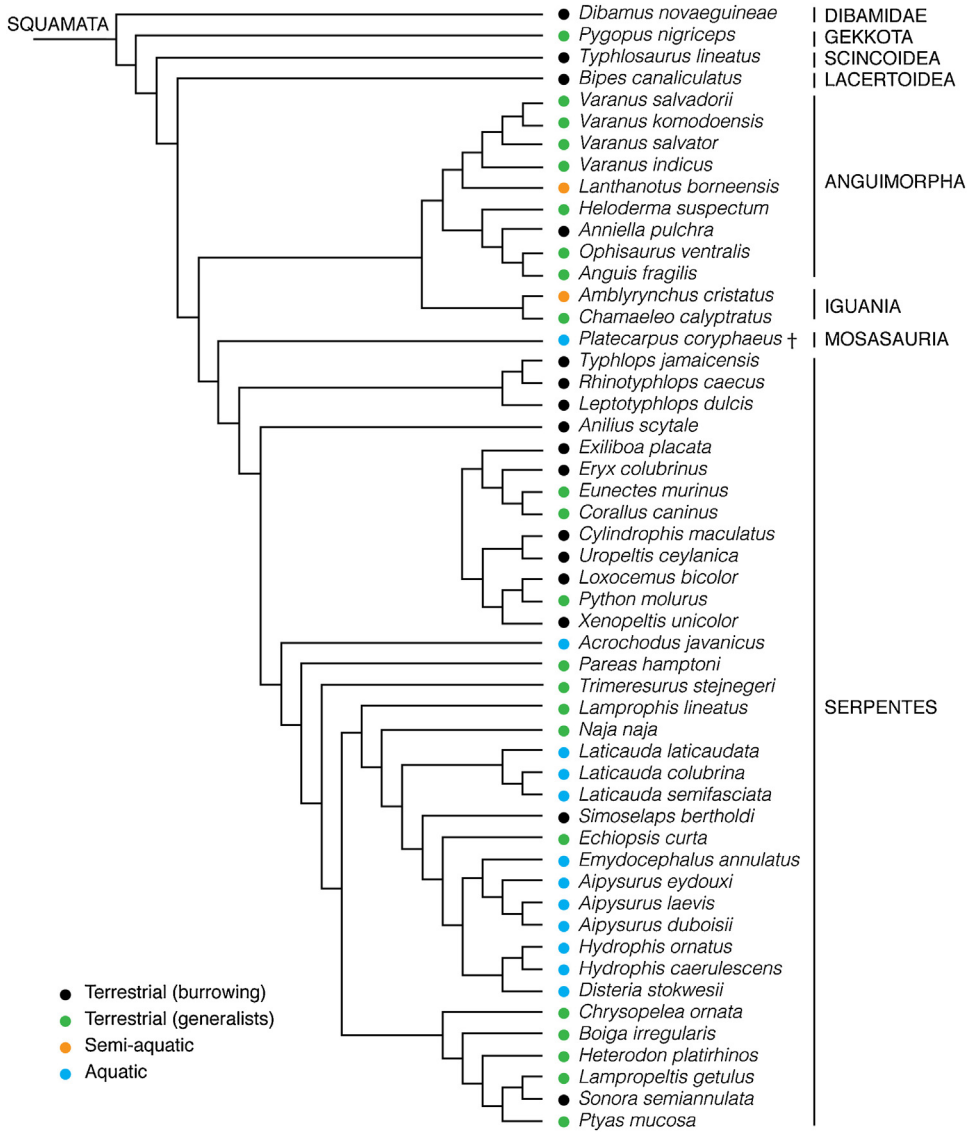

Fig. 2. Phylogeny of squamate taxa sampled in this study. The cross sign denotes fossils.

3.2. *Morphological descriptions of the bony labyrinth of* Platecarpus

The braincase of AMNH FARB1645 is nearly complete, with the alar process of the prootic damaged on both sides (Figs. 4 A, 5 A–D). It measures 160.52 mm wide between the tips of paroccipital processes, and 56.58 mm high from the damaged dorsal surface of the supraoccipital to the ventral margin of the basal tubercle of the basioccipital (Fig. 5A–D). Compared with non-mosasaurian squamates, the braincase of *Platecarpus* forms a triangular shape in dorsal view, with well-developed paroccipital processes extending posterolaterally.

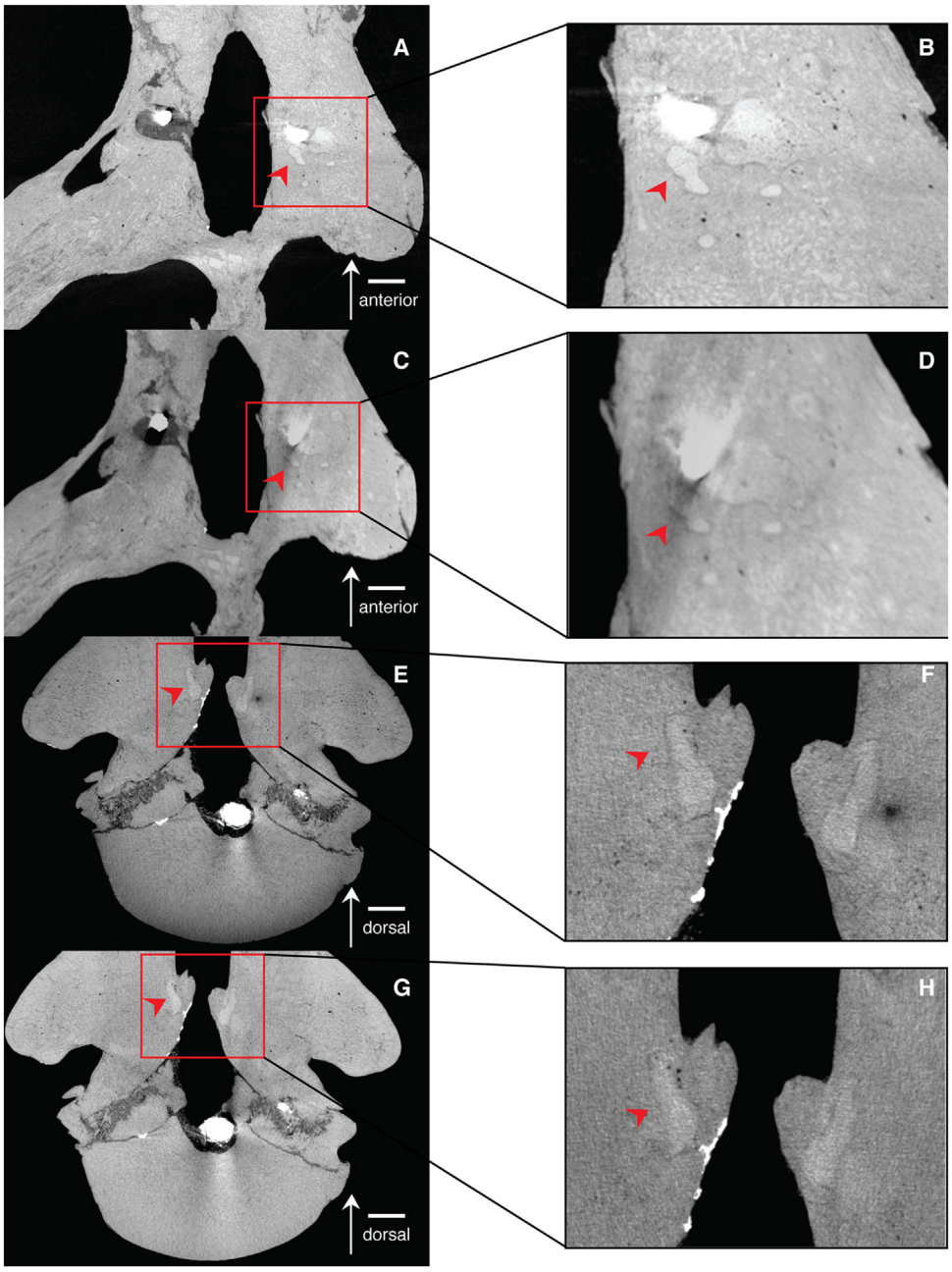

Fig. 3. Quality comparison of images from high-voltage and high-current scans. The red arrows denote the semicircular canals. (A, B) High-current scan of AMNH FARB1645. (C, D) High-voltage scan of AMNH FARB1645. (E, F) High-current scan of AMNH FARB1566. (G, H) High-voltage scan of AMNH FARB1566. Scale bar = 5 mm.

The bony labyrinth is preserved bilaterally inside the braincase, surrounded by the prootic, supratemporal, and the opisthotic that fuses with the exoccipital in AMNH FARB1645. In proportion to the braincase, the otic region is smaller in *Platecarpus* than those in extant aquatic and semi-aquatic squamates (Fig. 4). In dorsal view, the distance between the bony labyrinths is about 10% of the distance between the tips of the paroccipital processes (Fig. 5A, B). In posterior view, the height of the bony labyrinths is less than 25% of the height of the braincase (Fig. 5C, D).

In *Platecarpus*, the orientation of the bony labyrinth differs from the conditions in extant snakes and lizards. In AMNH FARB1645, the dorsoventral axis of the bony labyrinth, which goes through the common crus and the tip of the cochlea, tilts posteriorly from the sagittal plane of the braincase (Fig. 4A). This was not found in the extant samples whose dorsoventral axis is approximately parallel to the sagittal plane of the braincase (Fig. 4C–F). No obvious deformation is observed in AMNH FARB1645 that may have caused the otic regions to rotate without deforming the semicircular canals, so we report the posterior tilting of the inner ear as a unique character for *Platecarpus* until more evidence appears.

The bony labyrinth of *Platecarpus* consists of three slender semicircular canals surrounding a small vestibule with a flat

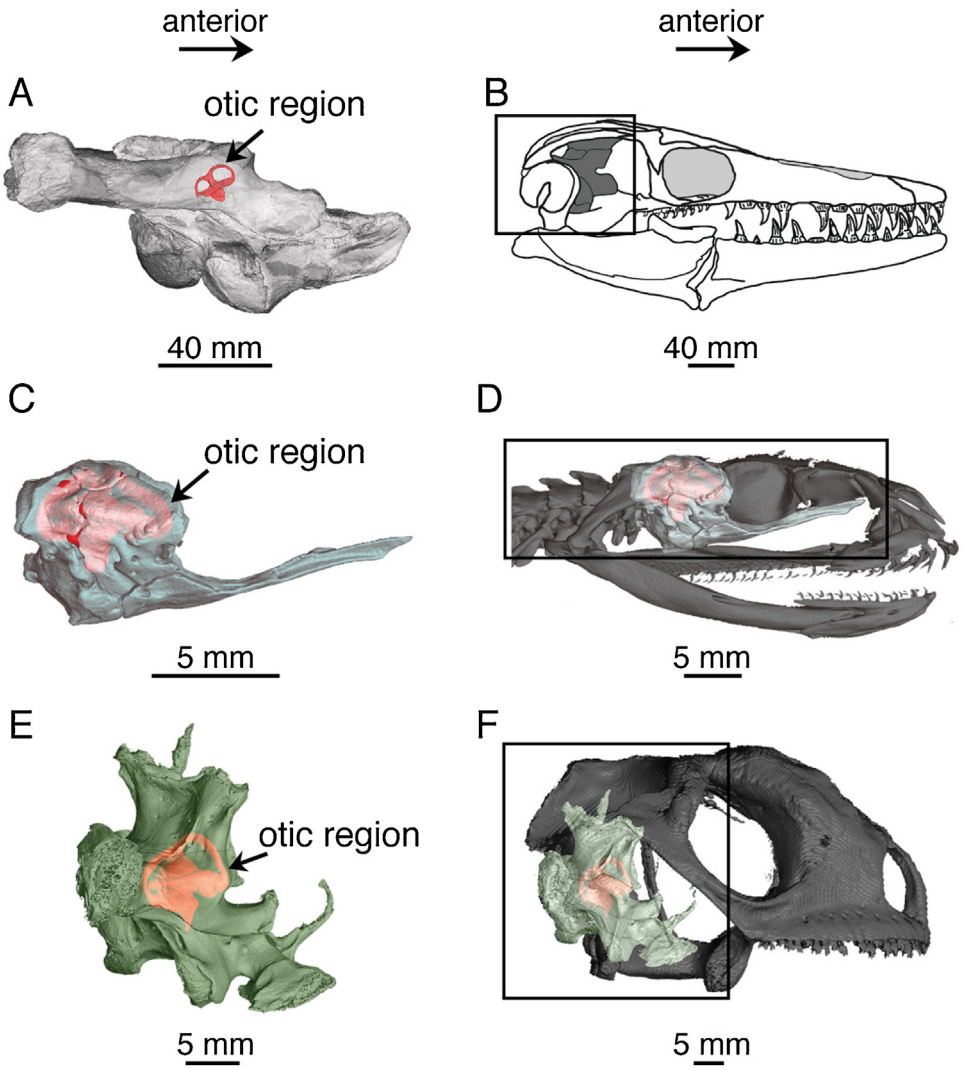

Fig. 4. Braincase of *Platecarpus* compared with extant aquatic and semiaquatic squamates. (A, B) Skull and braincase of *Platecarpus* in lateral view; line drawing of the braincase was modified from (Williston, 1898, pl. 13). (C, D) Skull and braincase of the *Aipysurus duboisii* in lateral view. (E, F) Skull and braincase of *Amblyrhynchus cristatus* in lateral view.

dorsal surface (Fig. 5E–J). Ventral to the vestibule is a well-developed cochlea resembling a reversed cone in shape. The anterior semicircular canal joins the posterior canal at the common crus. The lateral canal is connected with the posterior canal at its posterolateral margin. Each of the semicircular canals is connected with the vestibule through the ampulla. The semicircular canals are rounded in shape (Fig. 5E–J) — particularly the lateral semicircular canal, projecting far away from the vestibule when compared with other squamates (Fig. 6, first column). This resembles other mosasaurs (*Plioplatecarpus*, Cuthbertson et al., 2015) rather than modern sea snakes or the semi-marine Galapagos iguana, *Amblyrhynchus cristatus* (Fig. 6J–L).

The whole cochlear region of AMNH FARB1645 was reconstructed. It is proportionally larger in volume when compared with extant species, including the fully aquatic snake *Aipysurus laevis* (Fig. 6G–H), the semi-aquatic lizard *Amblyrhynchus cristatus* (Fig. 6J–L), the terrestrial lizard *Varanus indicus* (Fig. 6P–R), and the fossorial lizard *Bipes canaliculatus* (Fig. 6V–X). The dorsal portion of the cochlea bulges laterally (Fig. 6C) and connects to a sizable foramen ovalis (Fig. 5H). In modern sea snakes sampled in this study, the foramen ovalis is often reduced in size (Fig. 6D–I).

3.3. Size analysis of the bony labyrinth

Using phylogenetic generalized linear regression, we tested whether the length of the semicircular canals were smaller in *Platecarpus* than in extant species, in relation to the length of its skull. Data from extant samples supported a significant linear relationship between the length of the semicircular canals and the length of the skull, taking into account the phylogenetic relationships among the samples (Fig. 7). Each habitat group has species plotted above and below the regression line, and there is no clear trend where aquatic species have longer or shorter semicircular canals in the extant samples. A regression model was fitted to the extant data for each of the anterior, posterior,

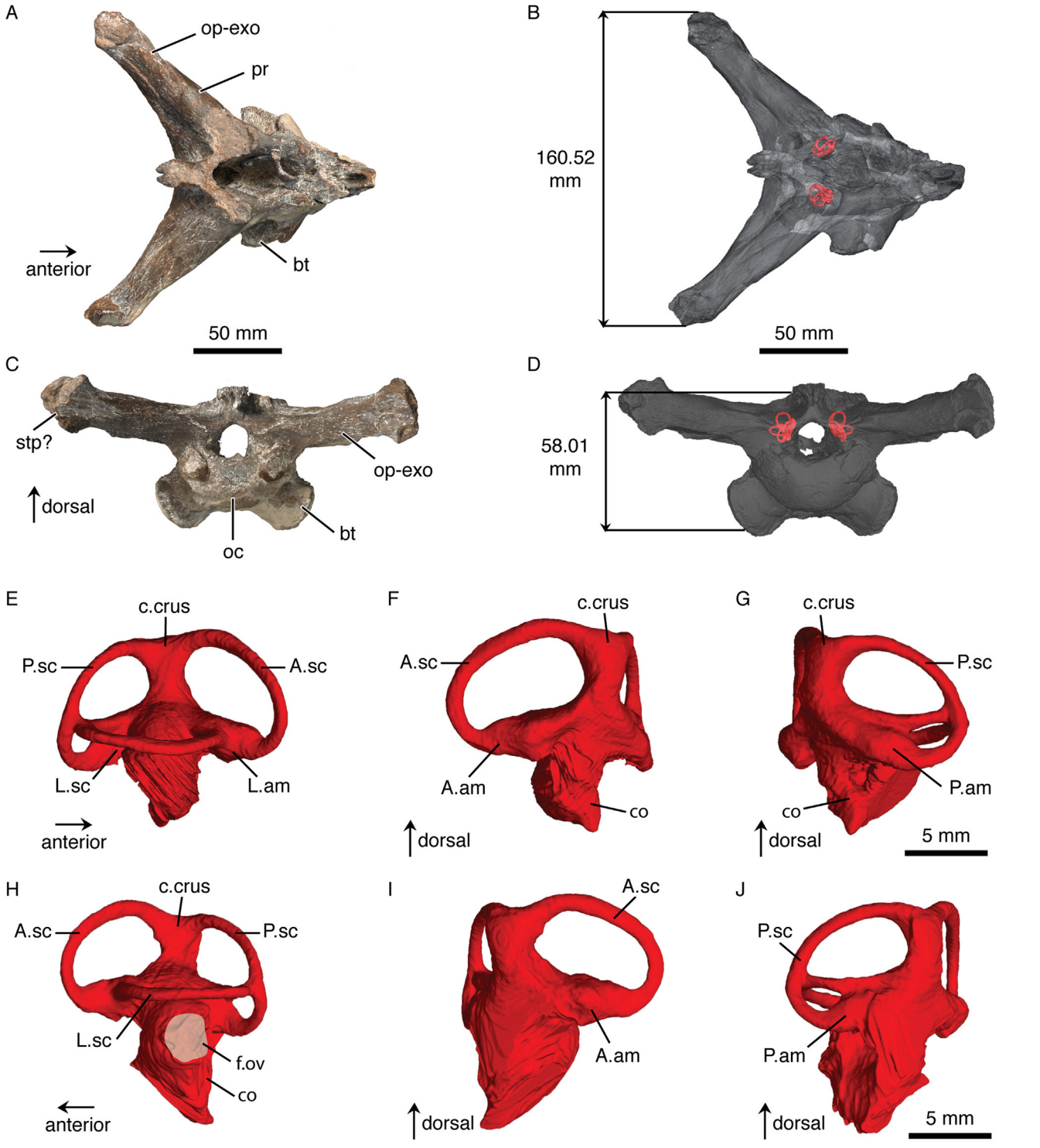

Fig. 5. The braincase and bony labyrinth of *Platecarpus* (AMNH FARB1645). (A–D) The specimen and virtual model of the braincase of AMNH FARB1645 are shown in dorsal (A, B) and posterior views (C, D). (E–G) The right bony labyrinth in lateral, anteromedial and posteromedial views. (H–J) The left bony labyrinth in lateral, anteromedial and posteromedial views. A.am, anterior ampulla; A.sc, anterior semicircular canal; bt, basal tubercle; c.crus, common crus; co, cochlea; f.ov, foramen ovalis; L.am, lateral ampulla; L.sc, lateral semicircular canal; oc, occipital condyle; op-exo, the fused opisthotic-exoccipital; pr, prootic; P.am, posterior ampulla; P.sc, posterior semicircular canal; stp, supratemporal.

and lateral semicircular canals. Based on the fitted model and the skull length of *Platecarpus*, prediction values and prediction intervals were calculated for the length of the semicircular canals. The results show that the fossil data were smaller than the predicted value, but they fell within the 95% prediction interval (Fig. 7). This means, in proportion to the skull, the semicircular canals in *Platecarpus* were not significantly shorter than those in extant squamates.

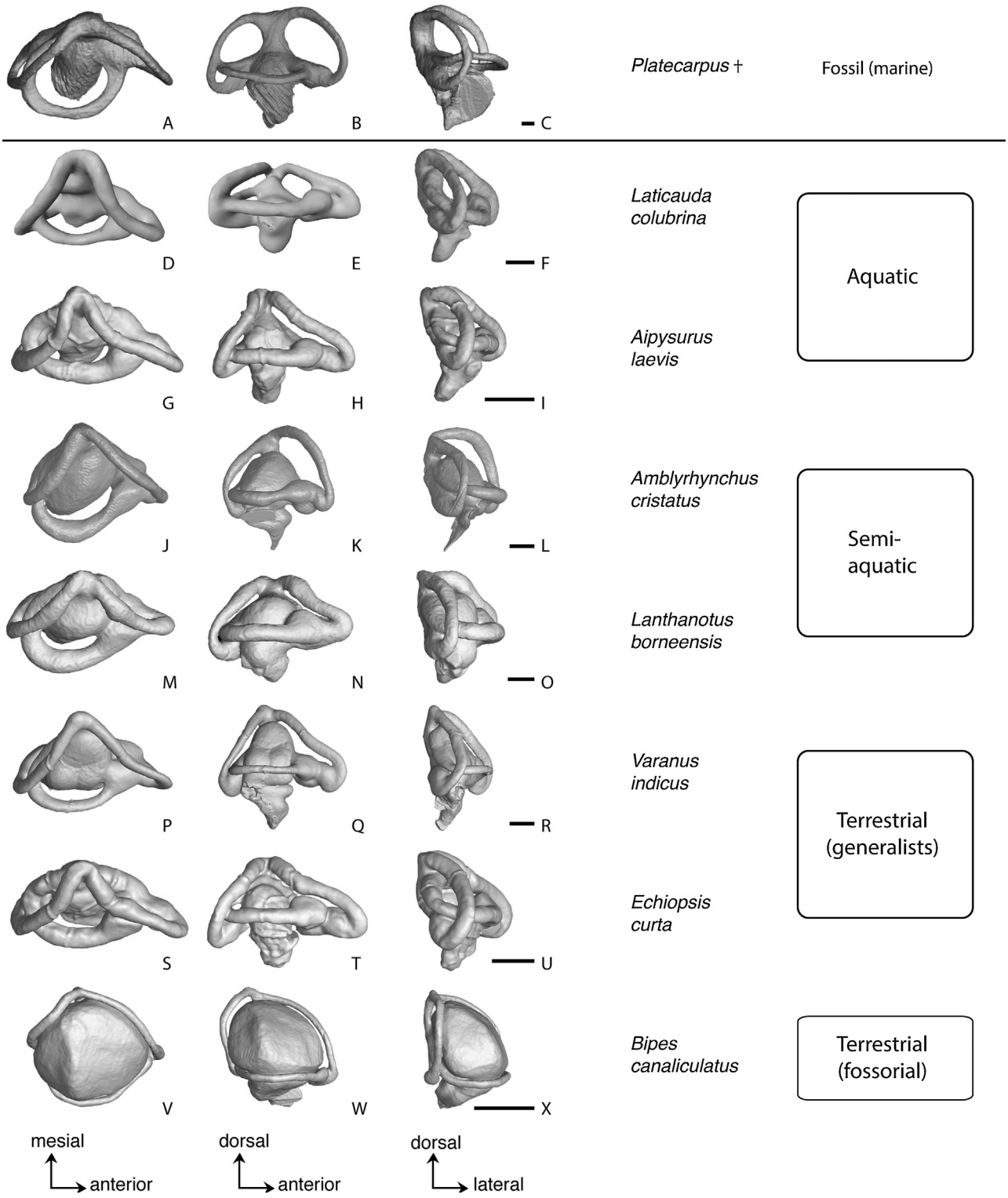

Fig. 6. The bony labyrinth of *Platecarpus*, a Cretaceous fossil genus, compared with the bony labyrinth of extant squamates inhabiting various environments. Left column of bony labyrinth models are in dorsal view, middle column, lateral view, and right column, posterolateral view. The *Platecarpus* bony labyrinth is reconstructed from AMNH FR1645. Specimen numbers of extant samples are listed in Table 1. Scale bar = 1 mm.

4. Discussion

As shown by the reconstructed CT models, slender and rounded semicircular canals distinguish mosasaurs from other squamates. This morphology has been found in *Platecarpus* (AMNH FARB1645) and *Plioplatecarpus* (Cuthbertson et al., 2015). The lateral semicircular canal almost forms a half circle, whereas in other squamates, the lateral semicircular canals are mediolaterally compressed (Fig. 6, first column). In extant lizards and snakes, the anterior and posterior semicir-

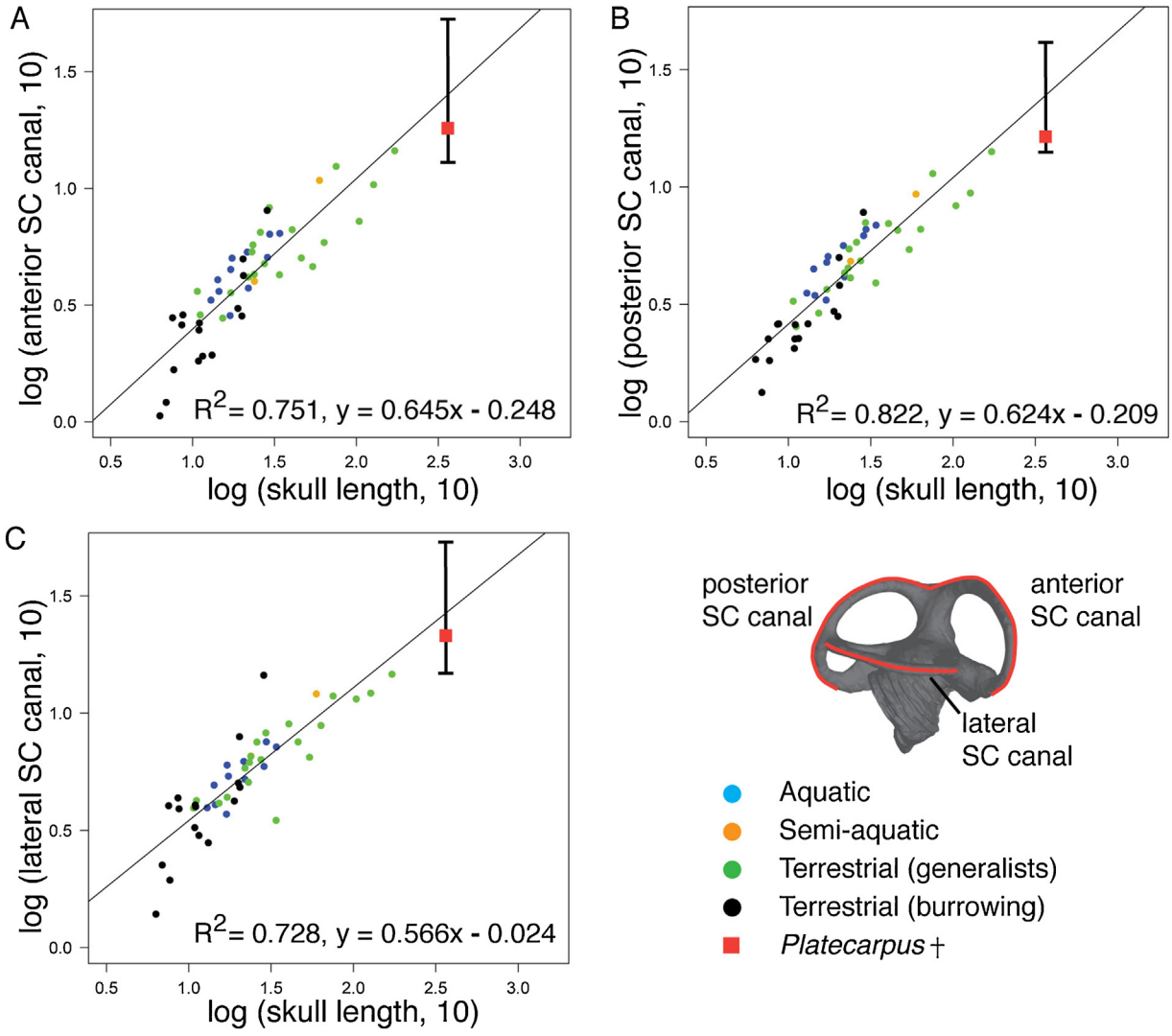

Fig. 7. Linear regression of the log-length of the semicircular canals to the skull. (A) Anterior semicircular (SC) canal. (B) Posterior semicircular (SC) canal. (C) Lateral semicircular (SC) canal. Bars in the regression plots denote the prediction interval of the length of the semicircular canals given the length of the skull. Colored dots are extant data; red squares are fossil data.

cular canals form a "pinched" morphology along the sutures of the supraoccipital to the prootic and the opisthotic (fused with the exoccipital), with both canals diverging further away from each other ventral to the sutures (Fig. 6, middle column). Different from this "pinched" shape, *Platecarpus* and *Plioplatecarpus* show rounded anterior and posterior semicircular canals arching smoothly at the sutures. When mapped on the phylogeny of Mosasauridae (sensu Bell and Polcyn, 2005), rounded semicircular canals first appeared in the common ancestor of *Platecarpus* and *Plioplatecarpus* (Fig. 8), yet with virtual models of mosasaur braincase accumulating (Polcyn, 2008), rounded semicircular canals may be found in more basal clades.

The functional significance of rounded semicircular canals is unclear for mosasaurs, due to the lack of modern squamates that share the same morphology. In mammals, size of the semicircular canals is often associated with agility — it has been established that cetaceans have smaller semicircular canals than terrestrial mammals (Spoor et al., 2002). In our analysis, the semicircular canals of *Platecarpus* were shorter than predicted by the linear model, but the observed data fell within the prediction intervals (Fig. 7). This is congruent with the previous analysis of the *Plioplatecarpus* inner ear (Cuthbertson et al., 2015). This suggests the size of the otic region was reduced in mosasaurs, but not to an extent that a functional inference could be made.

The reconstructed bony labyrinth of *Platecarpus* shows well-developed hearing apparatuses — the cochlea and foramen ovalis. The anteroposterior width of the foramen ovalis measures approximately half the width of the cochlea in lateral view (Fig. 5H). In contrast, size reduction is observed in the hearing apparatuses of several modern sea snakes, with the foramen ovalis forming a small opening dorsal to the cochlea (Fig. 6D-I). Lacking experimental data in extant sea snakes, it is difficult to compare their hearing ability with mosasaurs, but the morphological differences in their bony labyrinth indicate a diverse range of sensitivity to sound in marine squamates.

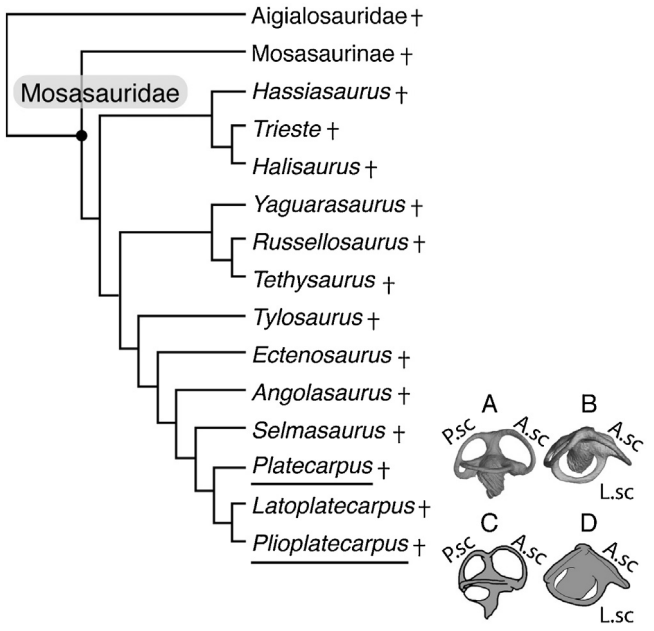

Fig. 8. Evolution of mosasaur inner ears, with the morphology of the bony labyrinth mapped on their phylogeny. The phylogeny is composited from Bell and Polcyn (2005) and Konishi and Caldwell (2007). (A, B) The right bony labyrinth of *Platecarpus* in lateral (A) and dorsal (B) view. (C, D) The right bony labyrinth of *Plioplatecarpus* in lateral (C) and dorsal (D) view, redrawn from Cuthbertson et al. (2015). A.sc, anterior semicircular canal; L.sc, lateral semicircular canal; P.sc, posterior semicircular canal. The cross sign denotes fossils. Reconstructed bony labyrinth models not to scale.

5. Conclusion

The reconstructed bony labyrinth of *Platecarpus* shows a large cochlea for processing sound. It also shows slender and rounded semicircular canals, resembling the semicircular canals of *Plioplatecarpus* but differing from those in extant squamates. Phylogenetic linear regression analyses of the fossil and extant data did not support mosasaurs having shorter semicircular canals when corrected with skull length. In all squamates sampled in this study, the length of semicircular canals is linear to the length of the skull. In contrast to the transition from land mammals to cetaceans, aquatic lifestyles may have affected the shape, rather than the size of the semicircular canals of mosasaurs.

Acknowledgements

We thank J. Thostenson, M. Hill, and H. Towbin at the Microscopy and Imaging Facility laboratory of the AMNH for help and training in CT scanning. The CT scans obtained from DigiMorph were supported by NSF grant EF-0334961 to M. Kearney and O. Rieppel, and we thank Dr. J. Maisano for accessing the data. We thank colleagues at the Herpetology Department of the AMNH for accessing the extant specimens. Mick Ellison provided excellent photographs of the mosasaur specimens. D. Sampath and S. Schoenfeld provided inspiring discussions. We thank Dr. Susan Evans and an anonymous reviewer for insightful comments that improved the quality of the manuscript. This project was funded by the Strategic Priority Research Program of the Chinese Academy of Sciences (XDA19050102, XDB18030504), the Chinese Academy of Sciences Pioneer Hundred Talents Program to H. Yi, the National Natural Science Foundation of China (Grant No. 41702020 and 41688103), The Macaulay Family endowment to M. Norell and the Division of Paleontology at the American Museum of Natural History.

References

Bell Jr., G.L., Polcyn, M.J., 2005. *Dallasaurus turneri*, a new primitive mosasauroid from the Middle Turonian of Texas and comments on the phylogeny of Mosasauridae (Squamata). Netherlands Journal of Geosciences — Geologie en Mijnbouw 84, 177–194.

Caldwell, M.W., Lee, M.S., 2001. Live birth in Cretaceous marine lizards (mosasauroids). Proceedings of the Royal Society, Biological Sciences 268, 2397–2401.

Conrad, J.L., 2008. Phylogeny and systematics of Squamata (Reptilia) based on morphology. Bulletin of the American Museum of Natural History 310, 1–182.

Cope, E.D., 1872. Catalogue of the Pythonomorpha found in the Cretaceous strata of Kansas. Proceedings of the American Philosophical Society 12, 264–287.

Cuthbertson, R.S., Maddin, H.C., Holmes, R.B., Anderson, J.S., 2015. The braincase and endosseous labyrinth of *Plioplatecarpus peckensis* (Mosasauridae, Plioplatecarpinae), with functional implications for locomotor behavior. The Anatomical Record 298, 1597–1611.

Felsenstein, J., 2004. Inferring Phylogenies. Sinauer Associates, Inc., Sunderland, Massachusetts, 664 pp.

Freckleton, R.P., Harvey, P.H., Pagel, M., 2002. Phylogenetic analysis and comparative data: a test and review of evidence. American Naturalist 160, 712–726.

Gauthier, J.A., Kearney, M., Maisano, J.A., Rieppel, O., Behlke, A.D.B., 2012. Assembling the squamate tree of life: perspectives from the phenotype and the fossil record. Bulletin of the Peabody Museum of Natural History 53, 3–308.

Georgi, J.A., 2008. Semicircular Canal Morphology as Evidence of Locomotor Environment in Amniotes. Doctoral Dissertation. Stony Brook University, Stony Brook, New York, 223 pp.

Greene, H., 2000. Snakes: The Evolution of Mystery in Nature. University of California Press, Oakland, California, 365 pp.

IUCN, 2017. The IUCN Red List of Threatened Species. Version 2017-3. http://www.iucnredlist.org, downloaded 2018.

Jones, G.M., Spells, K.E., 1963. A theoretical and comparative study of the functional dependence of the semicircular canal upon its physical dimensions. Proceedings of the Royal Society of London, Series B 157, 403–419.

Konishi, T., Caldwell, M.W., 2007. New specimens of *Platecarpus planifrons* (Cope, 1874) (Squamata: Mosasauridae) and a revised taxonomy of the genus. Journal of Vertebrate Paleontology 27, 59–72.

Lindgren, J., Caldwell, M.W., Konishi, T., Chiappe, L.M., 2010. Convergent evolution in aquatic tetrapods: insights from an exceptional fossil mosasaur. PLoS ONE 5, http://dx.doi.org/10.1371/journal.pone.0011998.

Pianka, E.R., Vitt, L.J., 2006. Lizards: Windows to the Evolution of Diversity. University of California Press, Oakland, California, 348 pp.

Polcyn, M.J., 2008. Braincase evolution in plioplatecarpine mosasaurs. Journal of Vertebrate Paleontology 28 (Suppl. 3), 128A.

Pyron, R.A., Burbrink, F.T., Wiens, J.J., 2013. A phylogeny and revised classification of Squamata, including 4161 species of lizards and snakes. BMC Evolutionary Biology 13, 93.

R Core Team, 2016. R: A Language and Environment for Statistical Computing. R Foundation for Statistical Computing, Vienna, Austria https://www.R-project.org/.

Reeder, T.W., Townsend, T.M., Mulcahy, D.G., Noonan, B.P., Wood, P.L., Sites, J.W., Wiens, J.J., 2015. Integrated analyses resolve conflicts over squamate reptile phylogeny and reveal unexpected placements for fossil taxa. PLoS ONE 10, http://dx.doi.org/10.1371/journal.pone.0118199.

Russell, D.A., 1967. Systematics and morphology of American mosasaurs. Bulletin of the Peabody Museum of Natural History 23, 1–241.

Sanders, K.L., Lee, M.S.Y., Bertozzi, T., Rasmussen, A.R., 2013. Multilocus phylogeny and recent rapid radiation of the viviparous sea snakes (Elapidae: Hydrophiinae). Molecular Phylogenetics and Evolution 66, 575–591.

Spoor, F., Bajpai, S., Hussain, S.T., Kumar, K., Thewissen, J.G.M., 2002. Vestibular evidence for the evolution of aquatic behaviour in early cetaceans. Nature 417, 163–165.

Wever, E.G., 1978. The Reptile Ear: Its Structure and Function. Princeton University Press, Princeton, New Jersey, 1024 pp.

Williston, S.W., 1898. Mosasaurs. University of Kansas Geological Survey 4, 83–221.

Yi, H., Norell, M.A., 2015. The burrowing origin of modern snakes. Science Advances 1, 1–5.